

# High-resolution fluvial record of late Holocene geomorphic change in northern Tunisia: climatic or human impact?

Dominik Faust<sup>a,\*</sup>, Christoph Zielhofer<sup>a</sup>, Rafael Baena Escudero<sup>b</sup>,  
Fernando Diaz del Olmo<sup>b</sup>

<sup>a</sup>Department of Physical Geography, Technical University of Dresden, 01062 Dresden, Germany

<sup>b</sup>Department of Physical Geography, University of Seville, 41004 Seville, Spain

Received 12 September 2003; accepted 13 February 2004

## Abstract

In Northern Tunisia the late Holocene alluvial record of Medjerda floodplain sediments indicates geomorphic changes due to fluctuations of past climate, superimposed by the effects of human activity. Geomorphic activity occurred several times, interrupting stable conditions. Enhanced fluvial dynamics occurred around 4.7, 3.0, 1.7, 1.0 and 0.7 ka cal BP. A peak of activity took place about 0.4 ka cal BP. Some periods of fluvial activity show event-like phenomena, in particular when an anthropogenic impact intensifies climatic aridification. This has been the case around 1.7, 1.0, 0.7 and 0.4 ka cal BP with severe floods in the Medjerda valley. During Antiquity as well as around 1.3, 0.8 and 0.5 ka cal BP immature alluvial soils have developed, the first one being the most distinct. Late Holocene Medjerda alluvial history shows that fluvial dynamics in Northern Tunisia were predominantly climate-driven. Anthropogenic impact only intensified or weakened these processes.

© 2004 Elsevier Ltd. All rights reserved.

## 1. Introduction

Geomorphological findings are vitally important in Quaternary palaeoclimatic and palaeoprocess research. In the past, they were primarily used as proxy data to define extensive Quaternary time scales, especially in loess–soil sequences (e.g. [Semmel, 1989](#)). Recently, geomorphic-sedimentological approaches have gained in importance even in high resolution stratigraphic records (e.g. [Zolitschka, 1998](#); [Dearing et al., 2001](#)). Geomorphic research increasingly focuses on Holocene climatic fluctuations (e.g. [Knox, 1993, 2000](#)). This study follows the theoretical approach of [Rohdenburg \(1989\)](#) by differentiating between geomorphic activity, semi-activity and stability. Rohdenburg's approach, which primarily helped to explain climatic fluctuations by means of morphodynamic changes within the glacial–interglacial cycle, may also be applicable to short-term Holocene climatic fluctuations in subtropical regions. Climate-driven geomorphic processes are mainly determined by water (precipitation), wind and landscape

sensitivity (relief, vegetation cover, pedologic and petrographic conditions). On the one hand, humid conditions result in a dense vegetation cover with soil formation and low surface runoff, resulting in landscape stability. On the other hand, arid conditions thin out vegetation and lead to fluvial and/or eolian activity (e.g. [White et al. 1996](#); [Rose et al., 1999](#)). A distinguishing feature for semi-arid regions is the high variability of precipitation with a generally high occurrence of excess rainfall and surface runoff events. Hence, subtropical geomorphic change reflects more the hygric than the thermal component of the climate. Geomorphic-sedimentological proxy data therefore provide an opportunity to complement the highly temperature-orientated approach in research of Quaternary climate change (e.g. [Johnsen et al., 1992](#); [Bond et al., 1997](#); [Cacho et al., 2000](#)) through valuable information concerning humidity at a regional scale (e.g. [Rose et al., 1999](#)).

When discussing and interpreting our own findings, it has been helpful to contextualise and compare them with other palaeoclimatic findings of regional (and global) scale. Nevertheless, we are dependent on palaeoclimatic records of various methods and tools (historical archives, pollen profiles, marine cores, coral reefs, speleotherms, alluvial sediments, etc.) taking into

\*Corresponding author. Tel.: +49-351-4633-4603; fax: +49-351-4633-7064.

E-mail address: dominik.faust@mailbox.tu-dresden.de (D. Faust).

account that the comparability of different archives is markedly limited. Correlations are always helpful and we suggested some in the course of this paper. However, correlations can only provide an indication—they will only seldom describe a cause-and-effect relation.

Land use change, due to political and socio-economic circumstances, reinforces the climatic effects on geomorphic processes (May, 1991; Faust, 1993, 1995; Oldfield, 2000). Historical sources, which provide information about the social situation of the population, are highly problematic in their palaeoclimatic interpretation for morphodynamics. Hsü (2000) emphasises that social crises may have the same effect as economic prosperity. For instance, historical archives document that within agrarian societies extensive migrations took place many times, triggered, for instance, by hunger and poverty. Often, they may correlate with a climatic downturn. Alternatively, warlike expansion (violent migration along with expulsion) occurred in times of abundance and cultural growth. Frequently, these periods correlate with climatic optima. Irrespective of the climatic conditions, both situations should initiate

active morphodynamics, provided that human impact predominantly determines geomorphic processes. In this study we intend to differentiate anthropogenic and climatic impacts on fluvial dynamics and to rule out their synergetic coactions.

## 2. Geographical setting

The central Medjerda basin (Fig. 1) in Northern Tunisia is a depression zone running in a west–east direction which has its origin in the Atlas orogenesis. Due to the low altitude of the basin (130–170 m above sea level) and dry winds, the meteorological station of Jendouba (143 m above sea level) records the maximum temperature of Tunisia. Average annual temperature is 17.8°C with a mean annual precipitation of 462 mm. With hot and dry summers and rainy winters the climate corresponds to the Mediterranean subtropics. According to Giessner (1984), the region is characterized by the transition from Mediterranean semiarid to semihumid conditions. This transition is ecologically documented

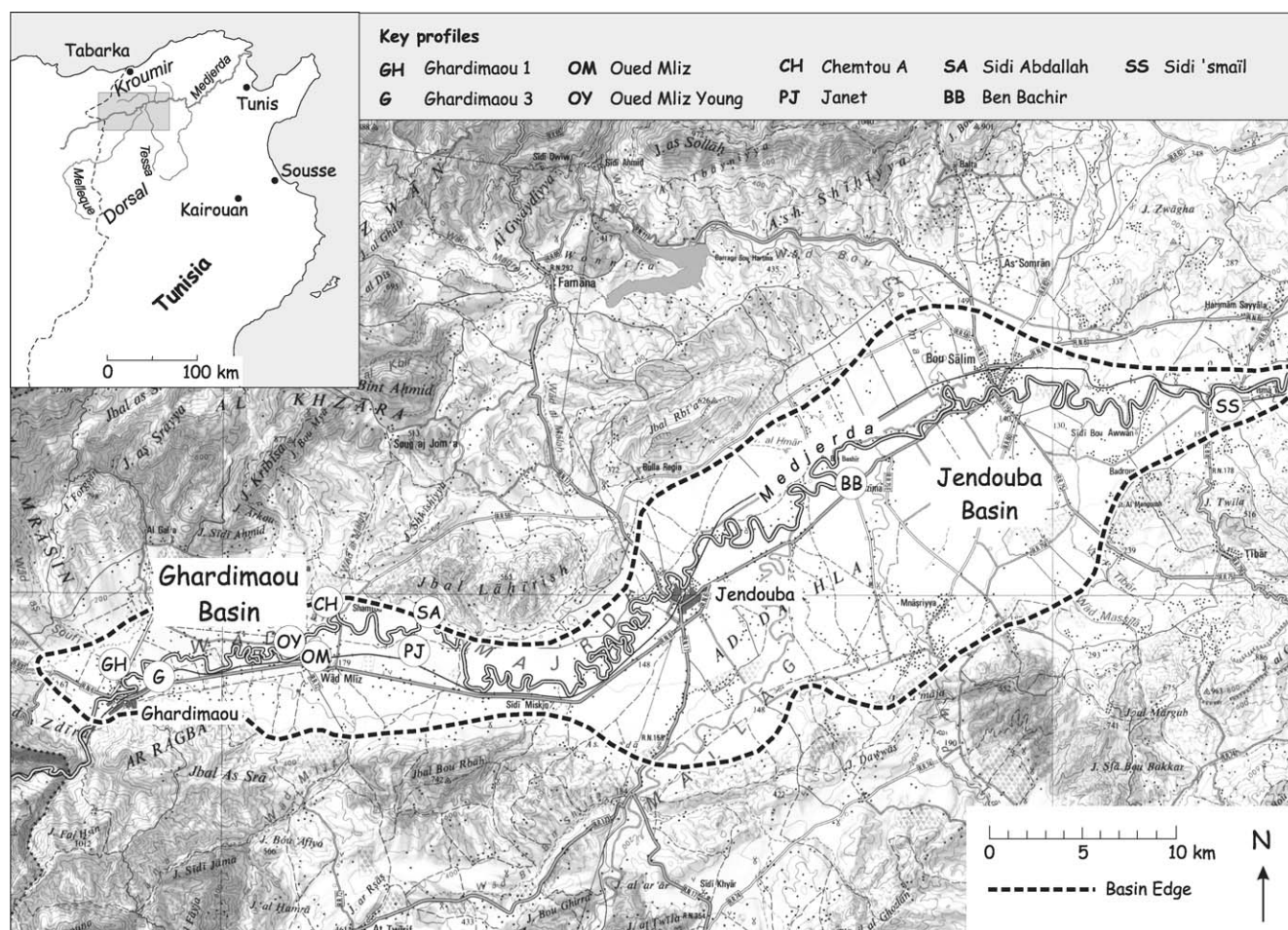


Fig. 1. Area of investigation.



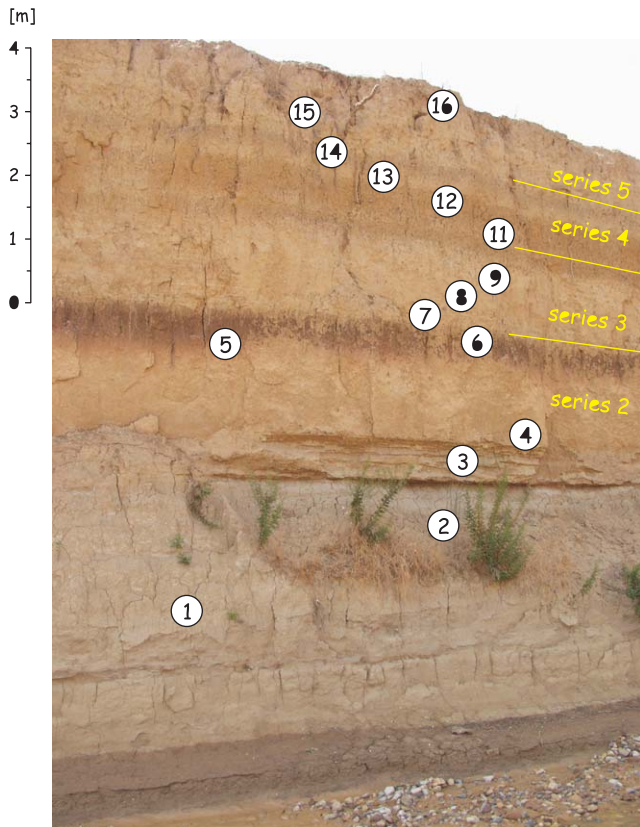


Fig. 2. OM profile in the Medjerda valley.

by the occurrence of the Mediterranean xerophytic forest with *Pinus halepensis* and shrubs of *Quercus ilex*. Due to strong anthropogenic superimposition, xerophytic forest is only to be found in recessional zones or protected areas.

The Medjerda River alluvial record shows changes in morphodynamics through weakly developed soils within the predominantly horizontally accumulated, fine-grained floodplain sediments. The sedimentation has taken place under rather stable circumstances, thus allowing the development of well-stratified layer sequences (Fig. 2). The meandering Medjerda River has incised into the 10 km wide Medjerda flood plain, which is filled up with Quaternary sediments. The meander belt exhibits an average width of 1–2 km. Due to the strong meandering, excellent exposures have developed, which made it possible to look at the sediments from very different angles and estimate the volume of each sediment layer.

### 3. Methods

#### 3.1. Field methods

We selected and sampled representative key profiles after examining the terrain for several months. The macroscale features of the key profiles provide a basis

for all subsequent analytic procedures. The stratigraphical units (“series”) were established during field examination. Charcoal samples of cultural layers and fireplaces represent well-dated in situ positions within late Holocene stratigraphical units. In addition artefacts and ceramic remnants have facilitated numerous dates.

#### 3.2. Sediment and soil analyses

We conducted Granulometry (cf. ISO/CD 11277), organic matter (cf. DIN 19684) and  $\text{CaCO}_3$ -content (Leser, 1977). At the exposure samples for thin section analyses were cut and taken orientated. To prepare the soil for thin section, excess moisture was removed by acetone exchange and impregnated with polyester resin. The sections were cut and polished to a size of  $3.5 \text{ cm} \times 2.5 \text{ cm} \times 20 \mu\text{m}$  to identify the micro-aggregate structure and morphology. For that purpose we used a standard polarisation microscope. The thin sections were observed under transmitted light and between crossed polars as well as under direct light until maximum 625-times magnified. Thin sections were carried out for the detection of initial soil formation (formation of soil aggregates), humification, biological activity, hydromorphic features, clay orientation by pressure, calcification, etc. In addition thin sections show clear features to distinguish in situ soil formation (micro-aggregation) from transported soil sediments (micro-bedded sediment structures).

#### 3.3. Palaeomagnetism

Palaeomagnetic samples were taken by means of a portable soft sediment corer (Baena Escudero, 1997). We measured natural remnant magnetisation (NRM), magnetic susceptibility and remnant magnetisation after demagnetisation. NRM was measured using a three axes cryogenic magnetometer (CCL-GM 4000). Magnetic susceptibility was measured with a susceptibility meter (KLY 2) and the demagnetisation using a Schonsted TSD-1-demagnetiser. All samples were selected and subjected to alternating field (AF) in steps from 0, 7.5, 10, 15, 20, 30, 50, 70 and 100 mT. When AF demagnetisation was applied to the samples in most cases the remnant magnetisation was fully neutralised by peak alternating fields of 70 mT. These results indicate that a low coercivity phase dominates the remanence. Natural remnant magnetization (NRM) intensities vary between 0.86 and 43 mA/m. Values of susceptibility range between 125 and 1773 ( $10^{-6}$  SI units). This relatively wide range is the result of the occurrence of soil horizons and the different content of calcium carbonate. In our investigation magnetic intensity ( $\text{mA m}^{-1}$ ), magnetic susceptibility ( $K_0 = 10^{-6}$  SI units) as well as inclination and declination ( $^\circ$ ) have been recorded.

### 3.4. Radiometric AMS $^{14}\text{C}$ and IRSL dating

In several cases charcoal pieces taken for AMS radiocarbon measurements are remnants of firesites and cultural layers, so luckily we can assume to have dated in situ material. Thirty samples have been processed by the AMS  $^{14}\text{C}$  laboratories in Kiel (KIA/Germany) and Miami (Beta/USA). Apart from fireplaces and cultural layers (in situ results) AMS radiocarbon measurements of charcoal pieces and humid acids were determined. All radiocarbon measurements were converted into approximate calendar years (cal BP) using the calibration curve of [Stuiver et al. \(1998\)](#). IRSL samples have been processed by the luminescence lab in Heidelberg (HDS). Because of high carbonate content and deficient bleaching only one IRSL sample gave significant result.

### 3.5. Anthracological analysis, determination of artefacts and ceramics

In total, 68 macro-remains were analysed at the Quaternary Wood Laboratory in Langlau (Switzerland). The determination of artefacts and ceramic remnants was carried out at the Geoarchaeological Institute of Seville University (Spain).

## 4. Results

### 4.1. Late Holocene centennial scale synthetic profile (Series 3–5)

Eight cut-side key profiles and one inner bank position (OY profile) reveal late Holocene fluvial sequences within the Medjerda basin ([Fig. 3](#)). Severe exposure examinations of overbank sediments allow classification into five sedimentation series, dividing the most distinct changes in fluvial dynamics. This paper describes three (late Holocene) sedimentation series: Series 3 sets in with a distinct fluvial activity after a longer period of soil forming process (omnipresent Neolithic soil closing Series 2; cf. [Zielhofer et al., 2004](#)). Series 3 ends with a distinct soil formation and/or the deposition of clayey to silty overbank-fines (GH, G, OM, CH, PJ, SA and SS profiles; [Fig. 3](#)). Relatively coarse sediments (loamy sand, coarse sand, gravels) indicate the beginning of Series 4 (e.g. GH, G, CH, PJ and SA profiles; [Fig. 3](#)). In some profiles, Series 4 ends with a weak soil formation or the deposition of clayey layers (e.g. GH, G, OM or CH profiles; [Fig. 3](#)). Series 5 is named “Youngest Layer” and is an ubiquitous deposition of fine laminated sediments in uppermost position (e.g. GH, G, OM, CH, PJ, SA, BA or SA profiles; [Fig. 3](#)). Thus, a series includes the sedimentation process and—if present—the following soil forma-

tion. Some of these series provide internal changes in texture and structure seen as interruptions of the sedimentation process which led to a subdivision (e.g. Series 3a–c). In some cases (cf. layer 8 of GH profile and layer 11 of G profile; [Fig. 5](#)) the correlated series do not provide the same granulometry due to different sedimentation environments of the meandering river (the coarser the sediment the nearer the channel lag).

Chronostratigraphical correlations (field and lab works,  $^{14}\text{C}$  dating, artefacts) make it possible to develop a high resolution synthetic profile representing late Holocene flood plain history ([Fig. 4](#)). This synthetic profile records alluvial series from 4.7 ka cal BP onwards and completes the Late Pleistocene to mid-Holocene findings of [Zielhofer et al. \(2004\)](#). For a further understanding of fluvial dynamics within the Medjerda flood plain we may refer to the works of [Faust and Zielhofer \(2002\)](#), [Zielhofer et al. \(2004\)](#) as well as [Zielhofer and Faust \(2004\)](#).

### 4.2. Palaeomagnetic record

[Fig. 5](#) demonstrates palaeomagnetic records from OY, GH and G profiles for the last 2000 years. Because of significant similarity with already published secular variation curves from central Europe and the Mediterranean region (cf. [Tanguy et al., 1985, 2003](#); [Clark et al., 1988](#); [Bucur, 1994](#); [Evans, 1996](#); [Gallet et al., 2002](#)) our declination and inclination values give major chronological information about flood plain evolution during the last two millennia. Tunisian inclination values mainly correspond with the inclination curve from Sicily (cf. [Tanguy et al., 2003](#); [Fig. 5](#)), whereas magnetic records from central Europe logically show higher inclination values (cf. [Clark et al., 1988](#); [Bucur, 1994](#); [Fig. 5](#)).

### 4.3. Sedimentation rates

On the basis of chronological findings (palaeomagnetism,  $^{14}\text{C}$  data) and corresponding sediment thickness of GH, G, OM, CH, PJ, SA, and SS profiles we can reconstruct a curve for the late Holocene average sedimentation rate within the Medjerda flood plain ([Figs. 5 and 6](#)). In doing so, the sedimentary conditions between two chronologically well-known marks are regarded as homogeneous. The sedimentation histories of BB profile and OY profile are ignored in the calculation: because the chronological resolution of alluvial units in the BB profile is unsatisfactory, and the OY profile documents sedimentation processes of an inner bank. Inner bank sedimentation rates reveal a different fluvial process, which is not comparable to moderate sedimentation of overbank fines.

Records of individual key profiles ([Fig. 3](#)) as well as chronostratigraphical conclusions and sedimentation

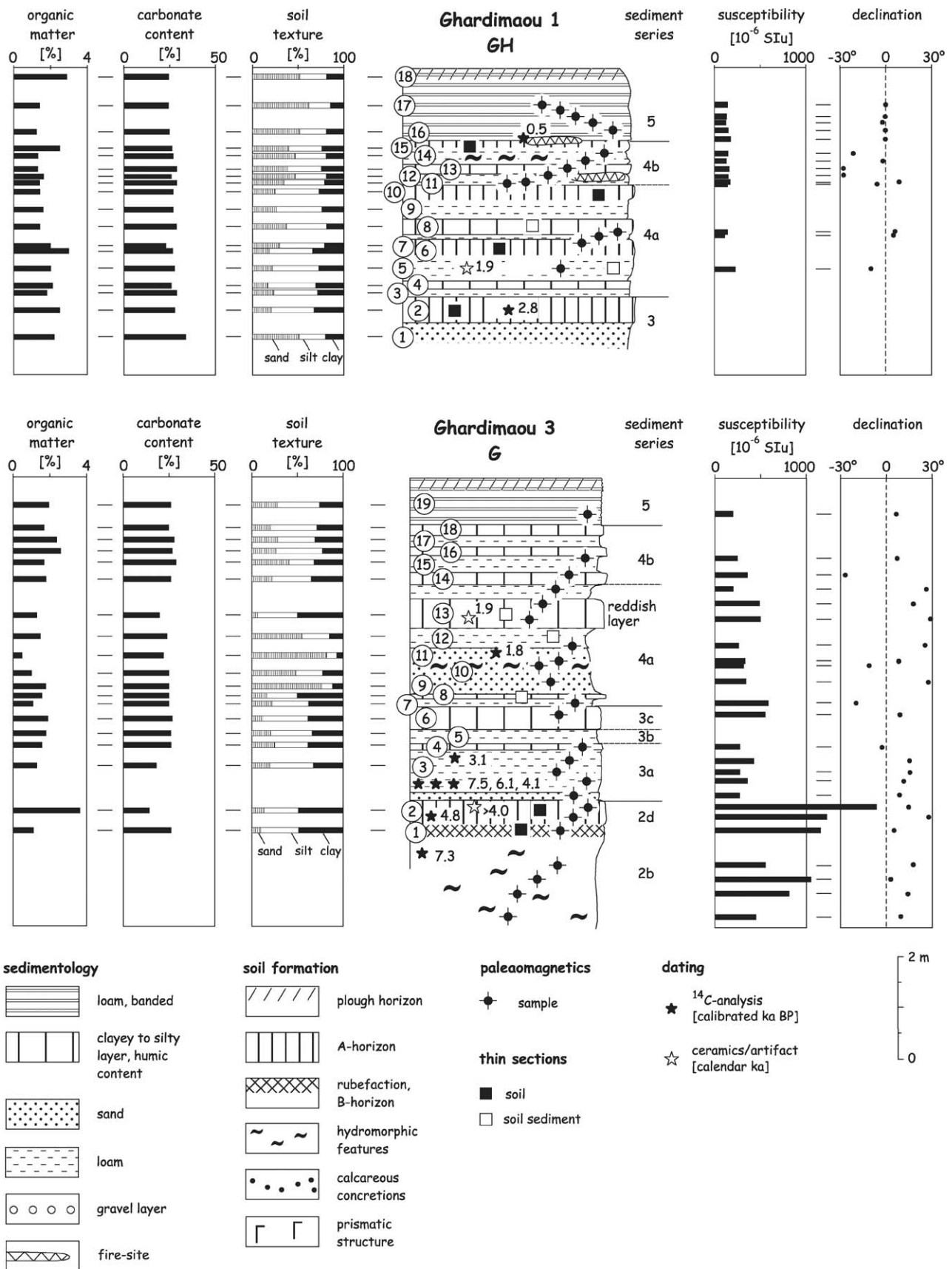


Fig. 3. (a–e) Key profiles and sediment series in the Medjerda Basin.

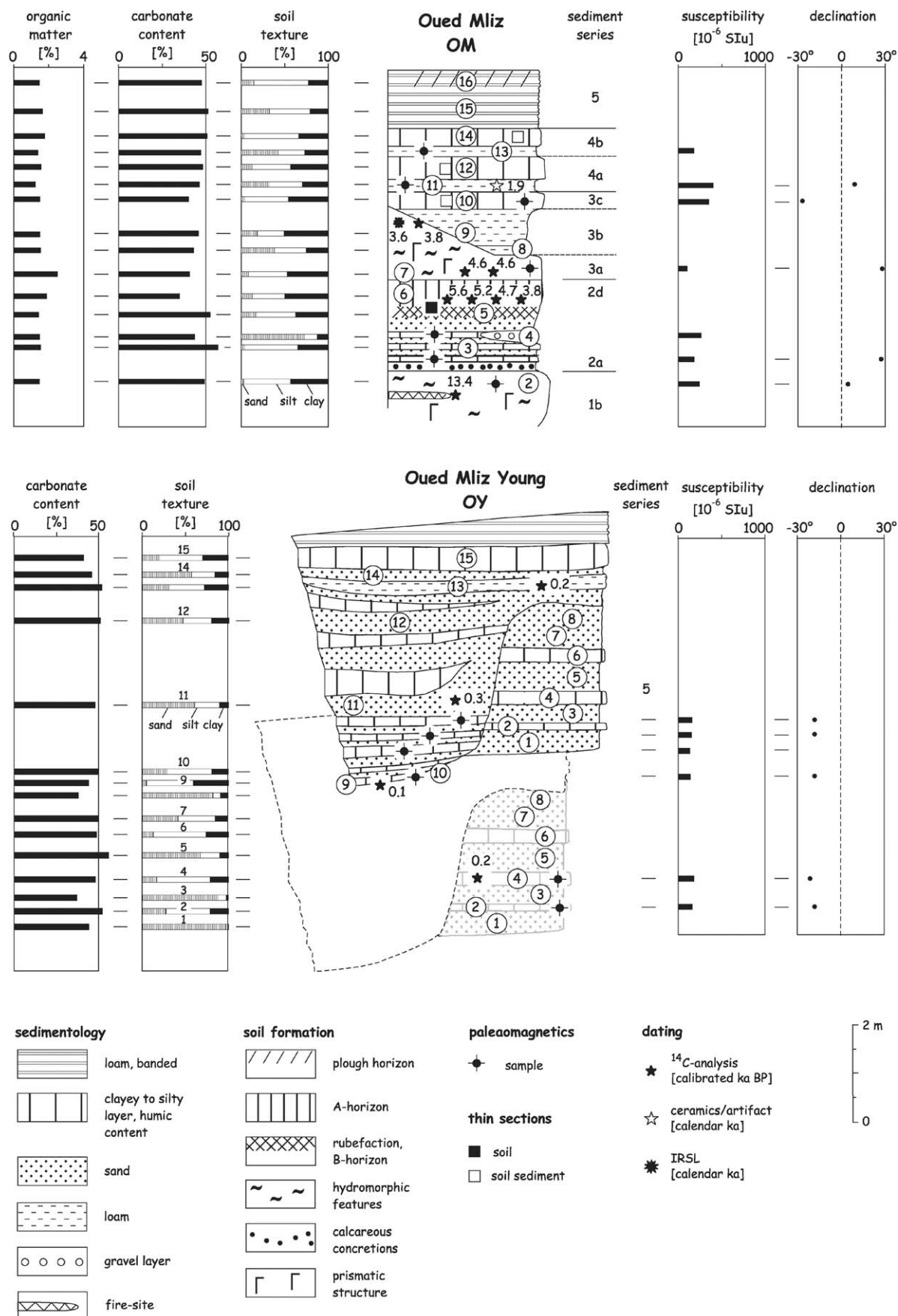


Fig. 3 (continued).

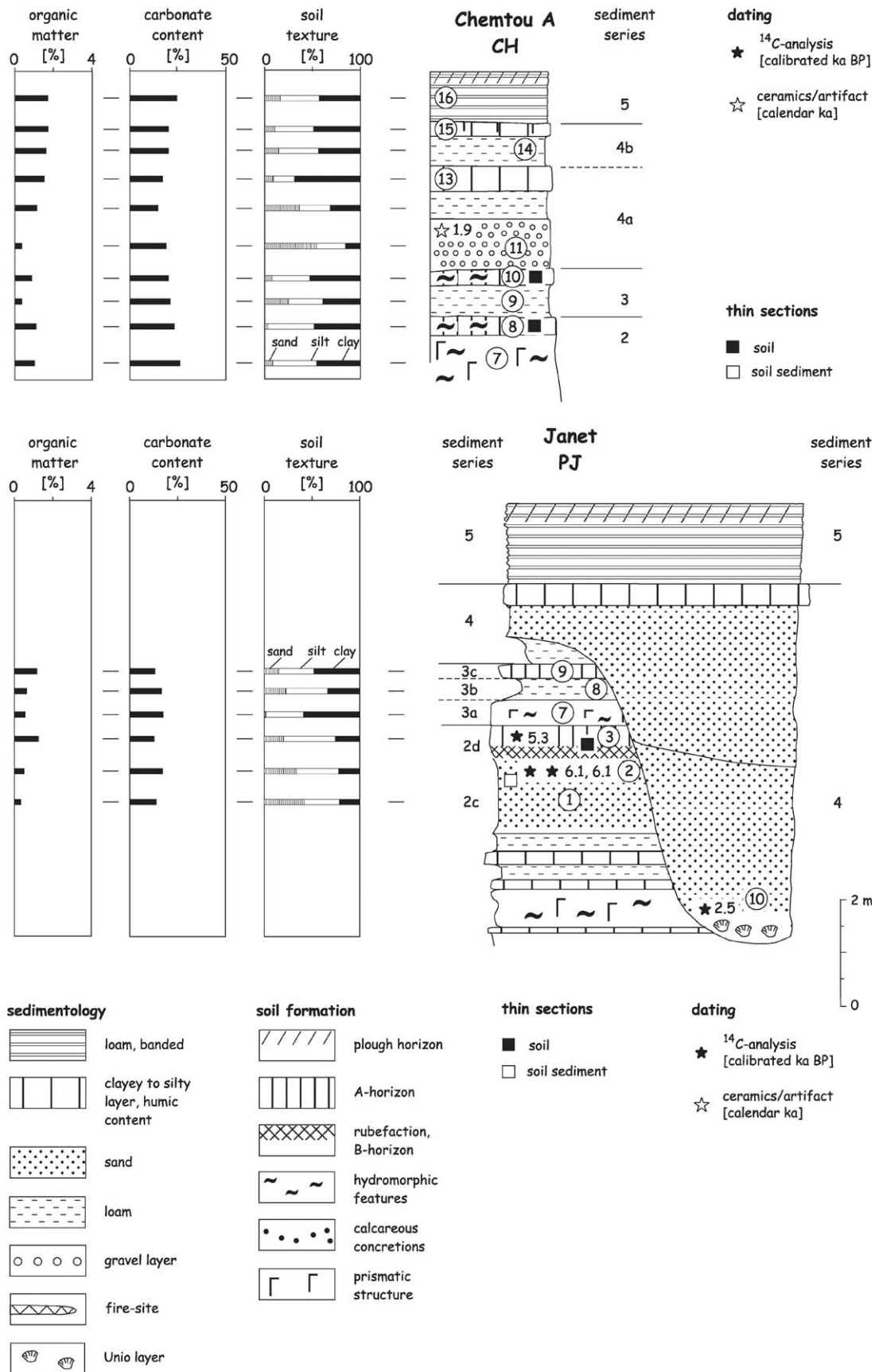


Fig. 3 (continued).

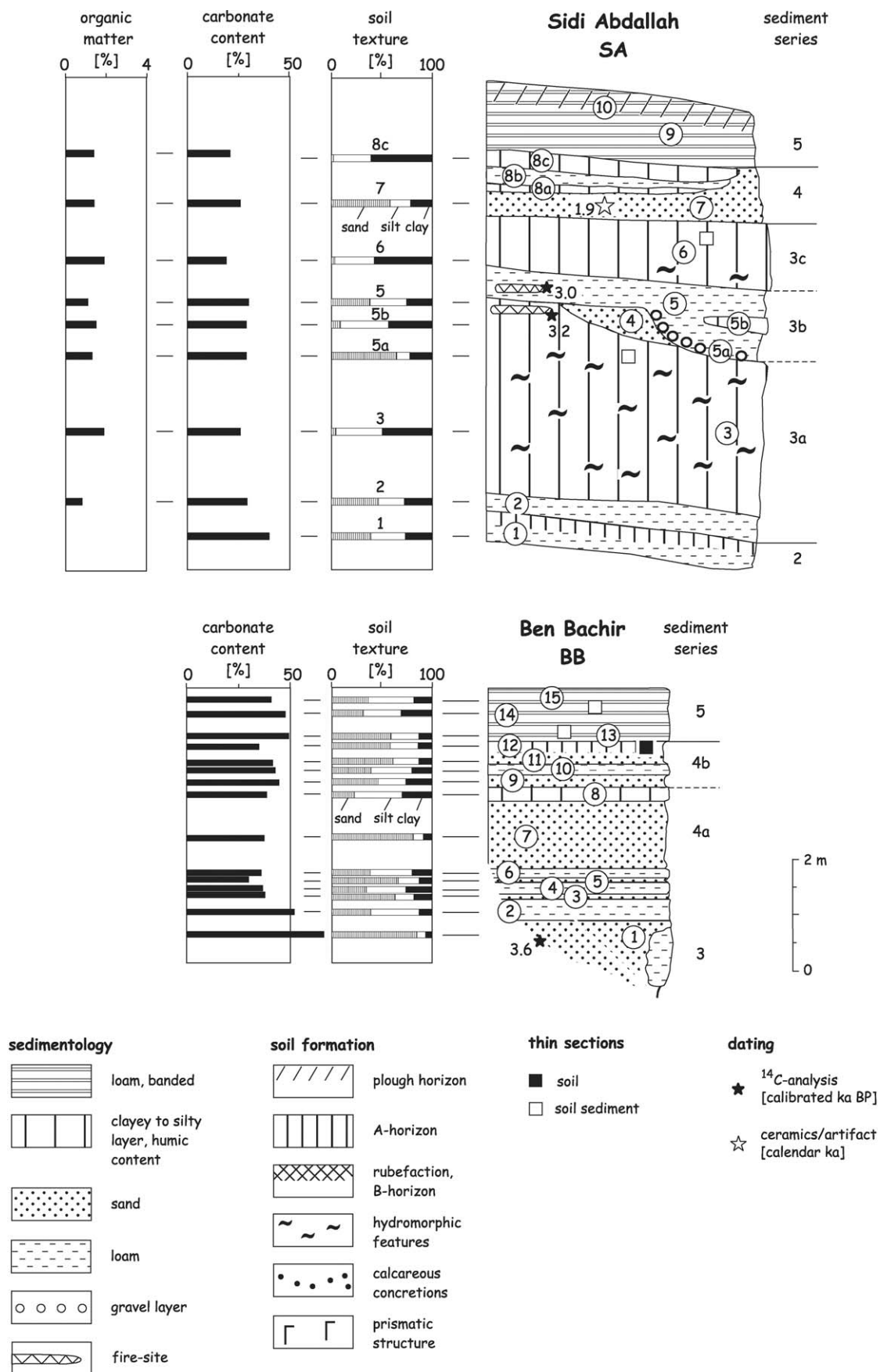


Fig. 3 (continued).



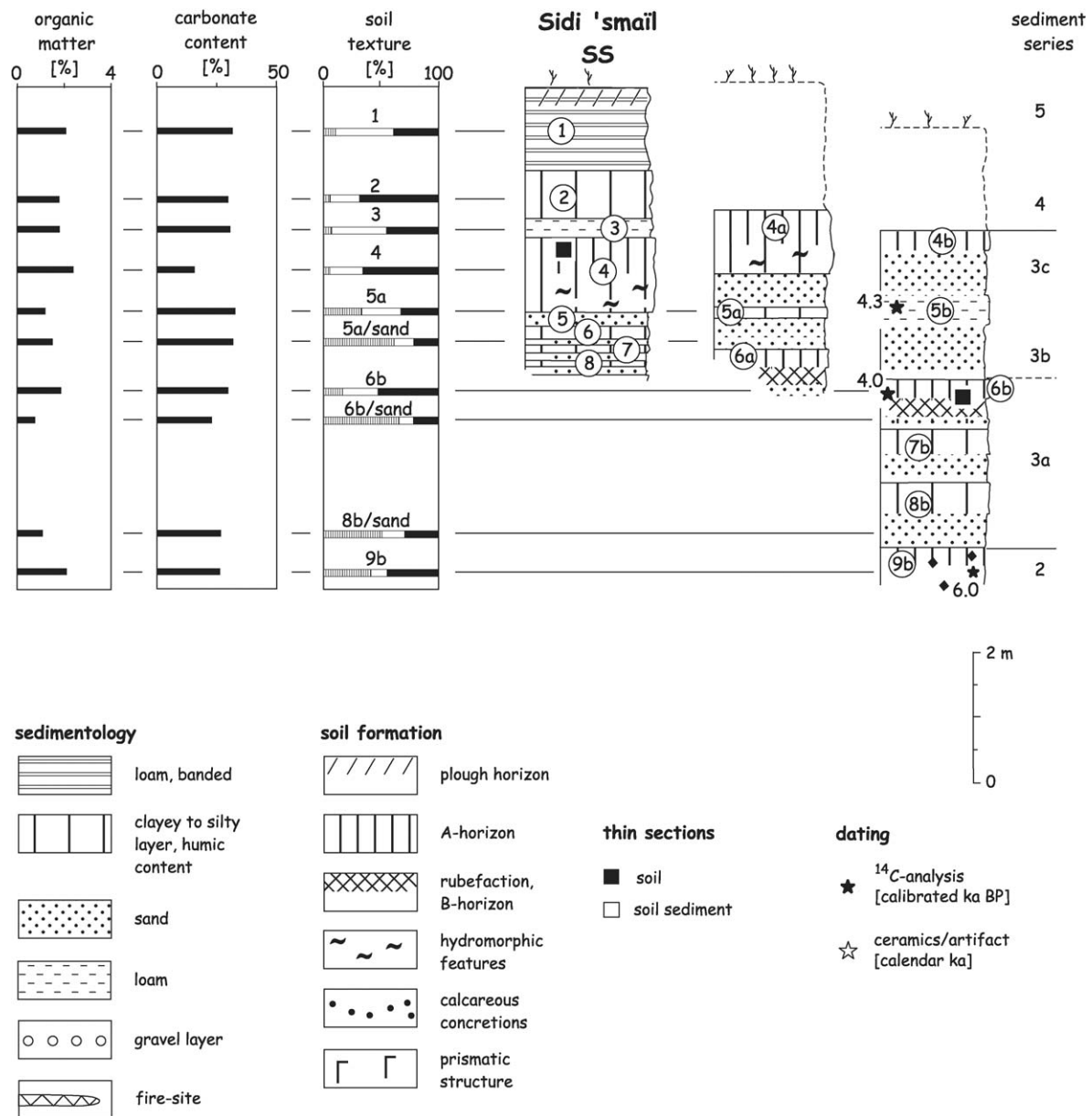


Fig. 3 (continued).

rates (Fig. 4) give detailed information about late Holocene alluvial history:

#### 4.4. Series 3a: 4.7–3.1 ka cal BP

After a strong mid-Holocene soil formation (cf. Zielhofer et al., 2004)—from 4.7 ka cal BP—a phase of enhanced fluvial activity sets in (Series 3), which can be observed in many layers within the Medjerda flood plain (e.g. SA2 ([SA=SA profile; 2=sample), CH9, thin sandy layer beneath G3, above SS9b; Fig. 3). In general, it involves quite coarse sediment layers above the mid-Holocene soil. However, there are exceptions as well. In OM and PJ profiles, the mid-Holocene soil (OM6 and

PJ3) is covered by very clayey fine sediments (OM7 and PJ7) with weak soil structure and hydromorphic features.

In some profiles, Series 3 ends with a fine-grained unit. It thus reveals traits of a fining-up sequence (GH1–GH2, OM8–OM10, CH9–CH10; Fig. 3). However, the most detailed Series 3 may be observed in SA profile: Series 3a begins with a sandy layer (SA2), which indicates enhanced fluvial dynamics. Primarily high sedimentation rates of Series 3a slowly decrease and the sedimentation becomes manifestly finer (SA3). This is a very fine-grained sediment (<5% sand), the content of clay and silt is almost equal. The thin section of the fine-grained SA3 layer shows hydromorphic features,

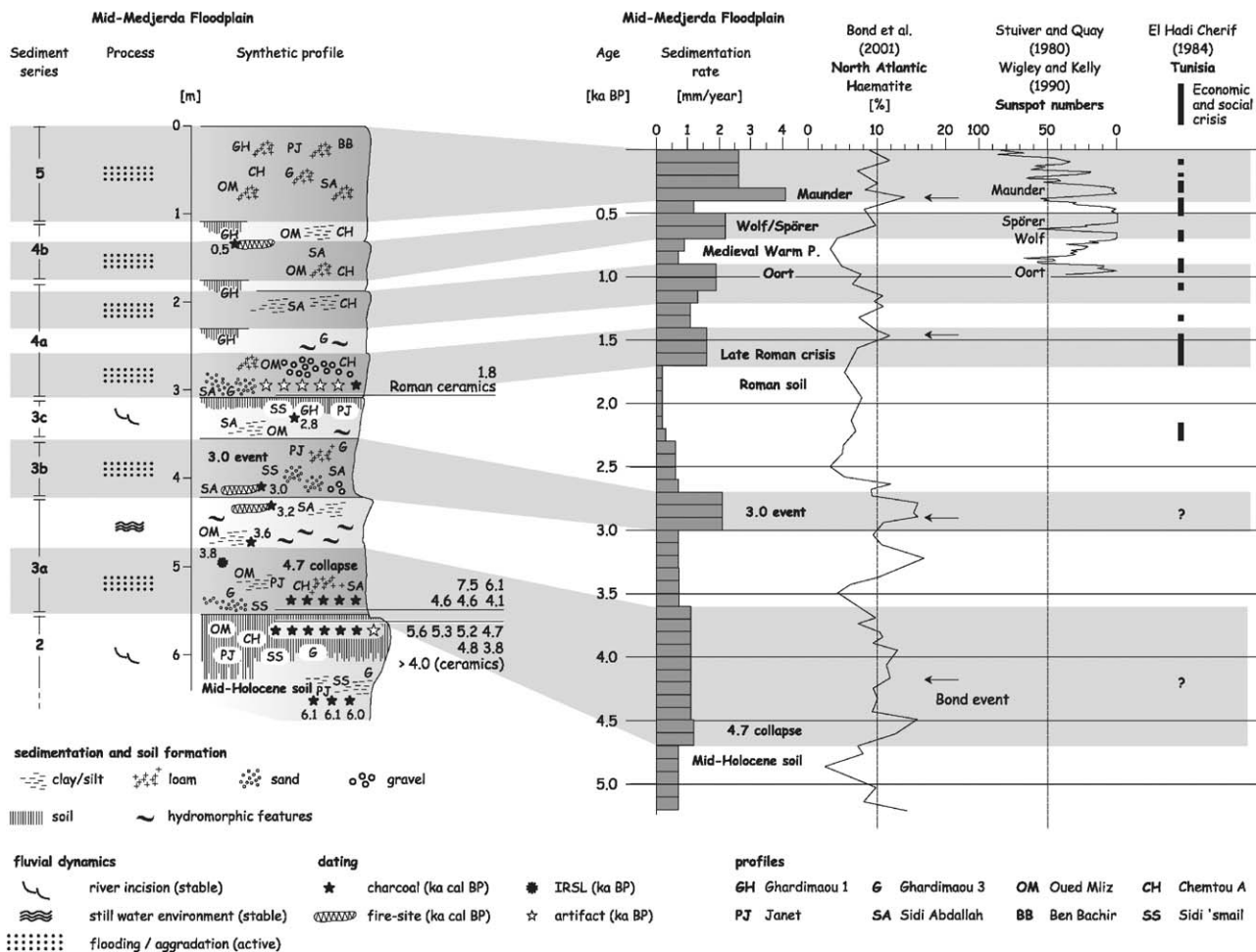


Fig. 4. Centennial scale synthetic profile.

probably induced by a contemporaneous rise of the groundwater level. Series 3a ends at around 3.1 ka cal BP, as a fireplace, directly below the top of SA3a layer, has been dated to 3.2 ka cal BP (Figs. 3d and 4). Beyond this fine deposition the Medjerda aggraded its channel with coarser material.

#### 4.5. Series 3b and 3c: aggradation from 3.0 ka cal BP

Series 3b begins with the aggradation of gravels and sandy components (SA4–SA5; Fig. 3d), pointing to increased fluvial activity. This Series 3b, which becomes gradually finer towards its top (SA5a: 65% sand; SA5: 40% sand), embeds a second fireplace (Figs. 3d and 4). The age can be specified to  $3010 \pm 130$  cal BP (3.0 ka event). Subsequently the sedimentation becomes fine-grained (Series 3c). Flood plain sediments (SA6) with a clay content of 60% are deposited. Thin section only shows weak hydromorphic features, which can be attributed to proceeding groundwater depression.

On the basis of the structure of the sediment sequence SA3 to SA6, it is possible to differentiate between 3a, 3b and 3c within Series 3. This sequence is also identifiable

in PJ profile (PJ7 to PJ9), SS profile (SS8b to SS4b) and in G profile (G3 to G6).

#### 4.6. End of Series 3: geomorphic stability until 1.7 ka cal BP

Within the Medjerda alluvial deposits clear pedogenetic features are developed only during longer periods of terrestrial conditions due to decreased groundwater table and/or decreased flood frequency. At the earliest from 2.8 ka cal BP (charcoal dating) on, more stable environmental conditions led to soil formation in GH profile (Fig. 3a). The thin section of GH2 shows precipitation crests of secondary carbonate, slightly etched carbonate grains and biopores. Additionally, more than 2% of organic matter and a distinguishable decrease of  $\text{CaCO}_3$  in this sample (GH2) indicate the formation of an A-horizon. The slightly decreasing carbonate content and increasing organic matter at CH profile (CH10; Fig. 3c) yield a comparable result. Furthermore, CH10 thin section reveals humification, initial rubefaction and calcified plant remains. Increased magnetic susceptibility and a relatively high oscillation

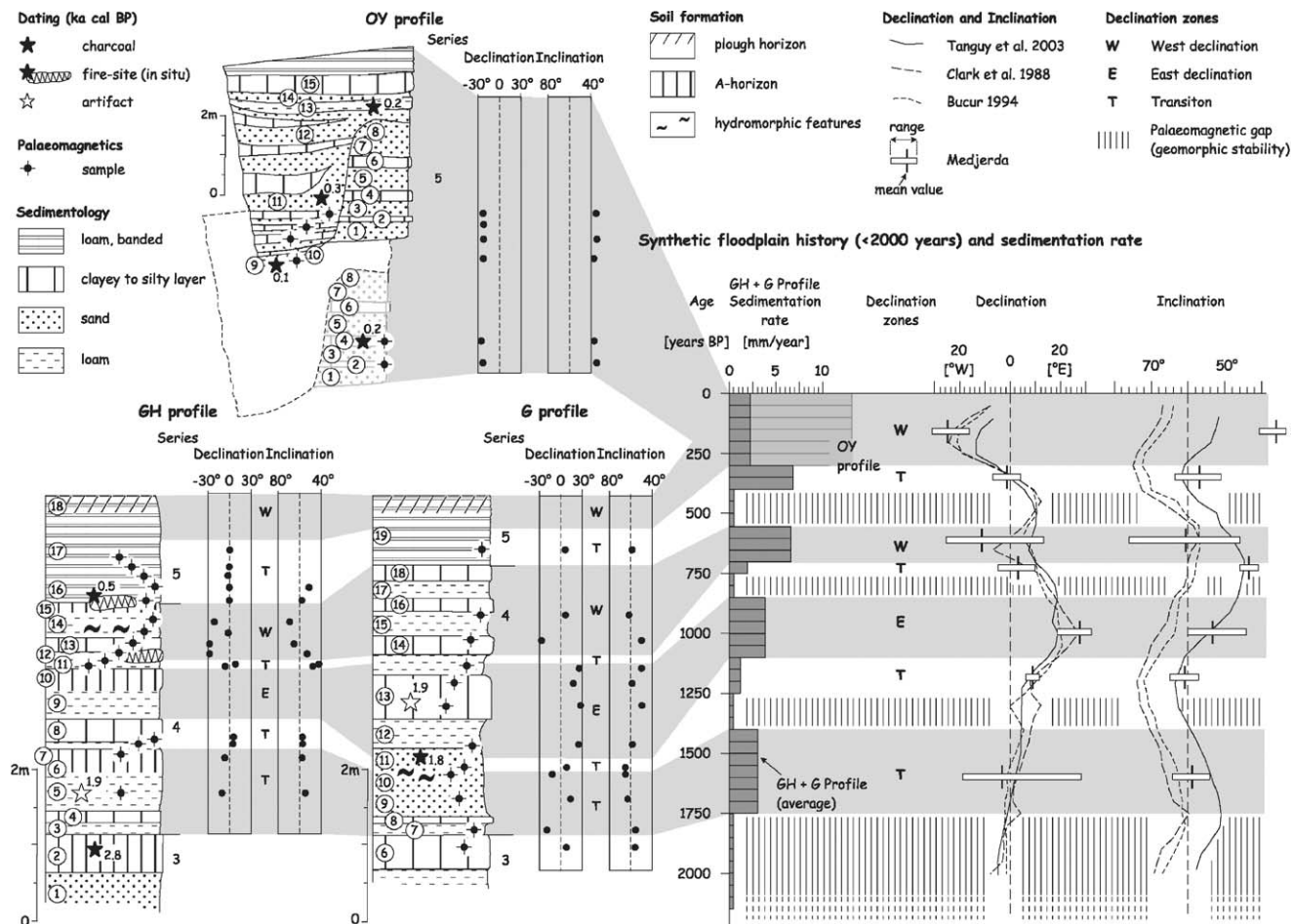


Fig. 5. Palaeomagnetism and chronostratigraphic correlation of GH, G and OY profile.

in declination values also suggest soil formation in G profile. G6 and G7 possess SI units [ $10^{-6}$ ] of  $> 500$  (Fig. 3a). At Sidi 'smaïl SS4 layer (Fig. 3e) also points to soil formation. SS4 thin section reveals a very homogenous matrix and initial rubefaction covering sandy grains.

During this pre-Roman to Roman soil formation the river incised (Fig. 4) to about 2–3 m above the contemporary Medjerda channel (Faust and Zielhofer, 2002; Zielhofer et al., 2002). Analyses of macro remains from the lowest part of the pre-Roman to Roman channel bed (PJ10; Fig. 3c) resulted in a range of plants (*Arbutus*, *Labiatae*, *Olea*, *Pistacia*), indicating a more humid climate than nowadays. A radiocarbon date yields an age of  $2550 \pm 190$  cal BP.

#### 4.7. Onset of Series 4a: enhanced aggradation from 1700 cal BP

At the end of the Roman period heavy floodings took place, which is recorded by an intense increase in sedimentation rate (up to 3.5 mm/year; Fig. 6) and relatively coarse deposits (Fig. 4). For the first time, the Medjerda River flooded the Roman settlement level.

Aggradations of gravels appear within the proximal areas of the river. However, CH11 cobble layer (Fig. 3c) is unequivocally derived from the Mellah River, a northern tributary of the Medjerda. The cobble layer is rich in Roman artefacts and broken marble from the nearby Roman quarry. In the G and SA profiles sandy layers are deposited (G9–G11, SA7; Fig. 3). These sediments show Roman ceramics (ordinary Roman ceramics and Sigillata A) as well. The post-Roman water level amplitude raised to values of about 8 m. Previously it rarely rose above the 5 m level (Faust and Zielhofer, 2002; Zielhofer et al., 2002). Late Roman to post-Roman overbank fines (GH3–GH7; Fig. 3a) include abundant molluscs of *Trochoida pyramidata* and *Pseudotachea splendida*, which signify drier conditions. While reddish layers in G and OM profiles (G13 and OM12) with their intense colouring resemble soils, the thin section clearly reveals micro-bedded sediment structures and, therefore, soil material deposited in a geomorphic active period.

During the late to post-Roman period of enhanced fluvial activity a short period of calm morphodynamics can be observed. Around 1.3 ka cal BP a short period of

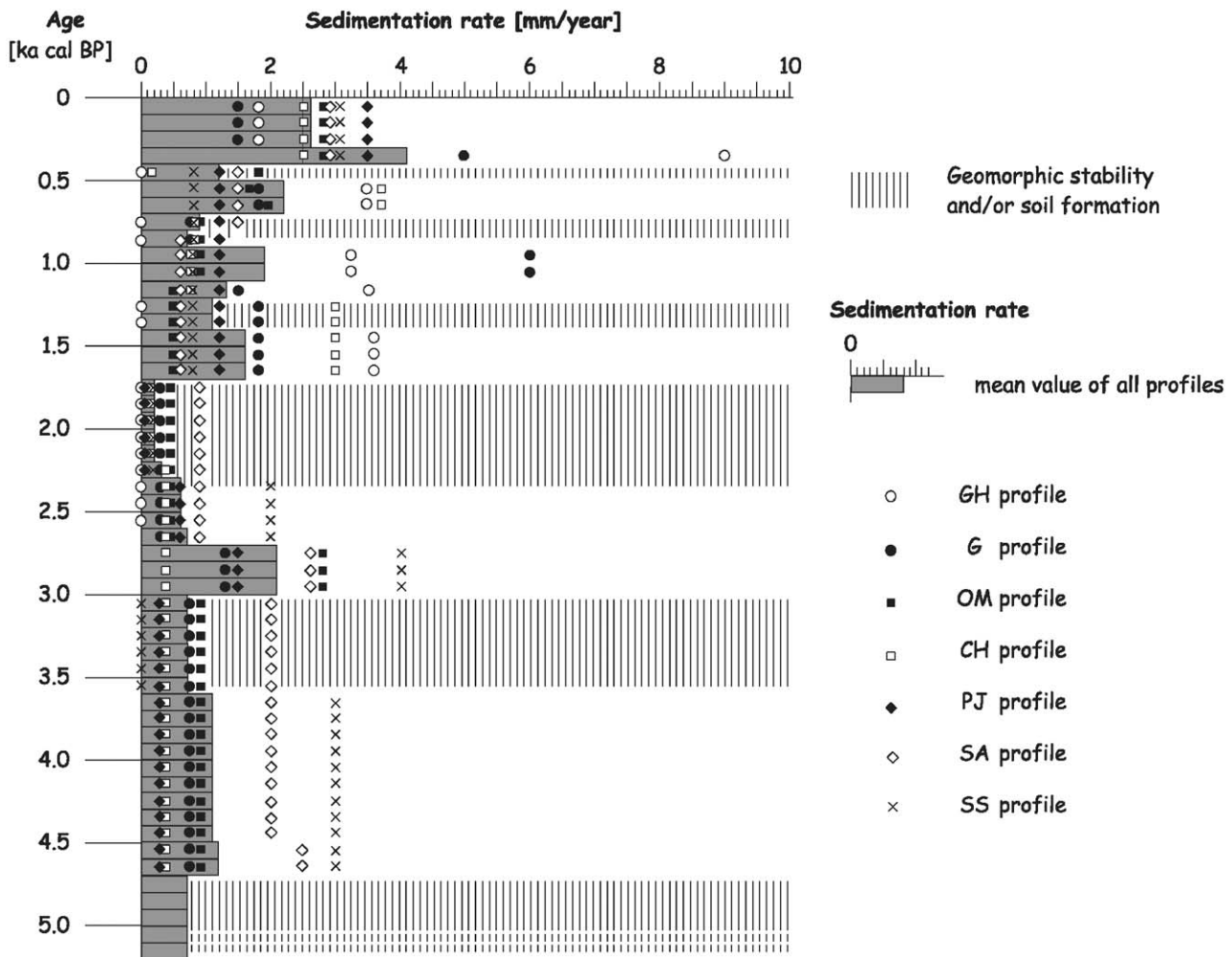


Fig. 6. Reconstruction of the average Medjerda sedimentation rate.

soil formation in the GH profile took place (GH6 and GH7; Fig. 3a). Carbonate content as well as the organic matter point to soil formation. The results from the thin section are even more distinct. The soil is well-aggregated and features numerous calcified plant remains. Because of bioturbation it is mixed well, resulting in a homogenous matrix. This early Medieval soil formation may possibly be observed only in GH profile. Probably at that time, GH profile was far away from the Medjerda channel due to a retreating meander loop. Therefore, the profile remained more or less unaffected by flooding. In this case, the early Medieval soil formation in GH profile does not represent an entire change in Medjerda fluvial dynamics.

#### 4.8. End of Series 4a: geomorphic stability and soil formation until 700 years BP

GH10 thin section shows humification and rubefaction, which signifies a clear soil formation (Fig. 3a). Fine-grained material (clay/fine silt) has been rinsed into the pores, gypsum crystals reveal relatively dry conditions.

The subsoil is just weakly rubefacted and only contains a few plant remains. Low declination and strong inclination values of the covering GH11 and GH12 layers correspond to the secular variation curve of Tanguy et al. (2003) and, therefore, give evidence that GH10 soil formation ends around 800 to 700 years BP (Fig. 5). At Sidi Abdallah (SA8a) and Chemtou (CH13) the deposition of fine-grained alluvial layers indicate low energy fluvial dynamics.

#### 4.9. Series 4b: fine-grained alluviation from 700 cal BP

A late Medieval fine-grained sedimentation, in almost each of the presented profiles, begins with clayey to loamy layers (GH11, G14, CH14, SA8b, BB9; Fig. 3) while their content of fine sand slightly increases in the course of time (GH12, G15). The late Medieval fine-grained sedimentation closes in some profiles with a weak soil formation (GH15, BB12, CH15; Fig. 3). In CH profile verification may have been already carried out macroscopically. It is a well-aggregated and humic soil matrix, which shows a gradual turn of colour



towards the subsoil. Even the biopores are macroscopically observable. BB profile reveals a poorly developed soil at the top of BB12, presenting slight brunification in the thin section. At Ghardimaou, colouring of GH15 layer shows slight brunification as well, which has also been proven in the thin section. Additionally, the thin section reveals carbonate fragments, rounded by solution, and bioturbation, thus abolishing former stratification. Accordingly, we assume a weak soil formation. A fire has then been lit on this ground. The  $^{14}\text{C}$

determination gives an age of  $497 \pm 32$  cal BP (Table 1 and Fig. 5).

#### 4.10. Series 5: youngest layer from 400 cal BP

All profiles of the mid-Medjerda valley close with an ubiquitous deposition of laminated sediments (Youngest Layer; Fig. 3). They indicate episodic flooding within the entire basin. Inclination and declination values of the Youngest Layer in GH profile point to an abrupt

Table 1  
Materials used for dating

| Profile                   | Layer/soil | Material                | Lab. no     | <sup>14</sup> C age (BP) | Calibrated age |           |
|---------------------------|------------|-------------------------|-------------|--------------------------|----------------|-----------|
|                           |            |                         |             |                          | Cal BP         | ka cal BP |
| <i>Radiocarbon dating</i> |            |                         |             |                          |                |           |
| GH                        | 15 (top)   | In situ fire-site       | Beta-135719 | 440 ± 25                 | 497 ± 32       | 0.5       |
| GH                        | 2          | Charcoal                | Beta-135720 | 2680 ± 46                | 2800 ± 60      | 2.8       |
| G                         | 11         | Charcoal                | KIA15295    | 1910 ± 25                | 1835 ± 95      | 1.8       |
| G                         | 3 (top)    | Charcoal                | Beta-135721 | 2940 ± 45                | 3105 ± 155     | 3.1       |
| G                         | 3 (bottom) | Humic acid              | KIA15296    | 3740 ± 70                | 4115 ± 235     | 4.1       |
| G                         | 3 (bottom) | Charcoal                | KIA15296    | 5280 ± 35                | 6055 ± 125     | 6.1       |
| G                         | 3 (bottom) | Charcoal                | KIA15297    | 6540 ± 40                | 7450 ± 120     | 7.5       |
| G                         | 2          | Charcoal (channel fill) | KIA15298    | 4195 ± 36                | 4750 ± 120     | 4.8       |
| G                         | 1 (bottom) | Charcoal                | KIA15299    | 6384 ± 83                | 7245 ± 215     | 7.3       |
| OM                        | 7          | Charcoal                | KIA15307    | 3510 ± 40                | 3765 ± 125     | 3.8       |
| OM                        | 7          | Charcoal                | KIA15308    | 4055 ± 35                | 4610 ± 200     | 4.6       |
| OM                        | 7          | Charcoal                | KIA15309    | 4074 ± 33                | 4625 ± 185     | 4.6       |
| OM                        | 6          | Humic acid              | KIA15304    | 3580 ± 90                | 3835 ± 235     | 3.8       |
| OM                        | 6          | Charcoal (channel fill) | KIA15306    | 4219 ± 37                | 4735 ± 125     | 4.7       |
| OM                        | 6          | Charcoal                | KIA15305    | 4519 ± 38                | 5175 ± 135     | 5.2       |
| OM                        | 6          | Charcoal                | KIA15304    | 4838 ± 39                | 5565 ± 95      | 5.6       |
| OY                        | 13         | Charcoal                | Beta-135722 | 250 ± 20                 | 235 ± 85       | 0.2       |
| OY                        | 11         | Charcoal                | Beta-135723 | 260 ± 20                 | 290 ± 140      | 0.3       |
| OY                        | 9          | Charcoal                | Beta-135724 | 150 ± 15                 | 135 ± 145      | 0.1       |
| OY                        | 4          | Charcoal                | Beta-135725 | 220 ± 20                 | 155 ± 155      | 0.2       |
| PJ                        | 10         | Charcoal (channel fill) | KI5014      | 2490 ± 30                | 2550 ± 190     | 2.6       |
| PJ                        | 3          | Humic acid              | KIA15286    | 4600 ± 80                | 5275 ± 325     | 5.3       |
| PJ                        | 1          | Charcoal                | KIA15286    | 5340 ± 35                | 6135 ± 145     | 6.1       |
| PJ                        | 1          | Charcoal                | KIA15285    | 5400 ± 150               | 6125 ± 375     | 6.1       |
| SA                        | 3 (bottom) | In situ fire-site       | KIA15074    | 2880 ± 30                | 3010 ± 130     | 3.0       |
| SA                        | 2          | In situ fire-site       | KIA15408    | 3000 ± 25                | 3200 ± 130     | 3.2       |
| BB                        | 1          | Charcoal                | KIA15303    | 3310 ± 25                | 3555 ± 80      | 3.6       |
| SS                        | 5b         | Charcoal                | KIA15320    | 3847 ± 28                | 4280 ± 130     | 4.3       |
| SS                        | 6b         | Charcoal                | KIA15072    | 3710 ± 30                | 4035 ± 115     | 4.0       |
| SS                        | 9b         | In situ Capsian layer   | KIA15073    | 5325 ± 30                | 6040 ± 130     | 6.0       |
| <i>Artefacts</i>          |            |                         |             |                          |                |           |
| Profile                   | Layer/soil | Material                | Epoch       |                          |                |           |
| GH                        | 5          | Ceramics                | Roman       |                          |                |           |
| G                         | 13         | Ceramics                | Roman       |                          |                |           |
| G                         | 2          | Ceramics                | Neolithic   |                          |                |           |
| OM                        | 11         | Ceramics                | Roman       |                          |                |           |
| CHA                       | 11         | Ceramics                | Roman       |                          |                |           |
| SA                        | 7          | Ceramics/marble         | Roman       |                          |                |           |
| SS                        | 9b         | Microliths              | Capsian     |                          |                |           |
| <i>IRSL</i>               |            |                         |             |                          |                |           |
| Profile                   | Layer/soil | Material                | Lab. no     | IRSL-age (ka BP)         |                |           |
| OM                        | 7          | Floodplain sediment     | HDS-1077    | 3.6 ± 0.7 maximum age    |                |           |

onset of Series 5 around 400 years BP (GH16–GH18; Fig. 5). Due to a marked incision of the Medjerda channel at that time, we have to expect a water level amplitude that exceeds 10 m (Faust and Zielhofer, 2002; Zielhofer et al., 2002). The constantly low declination values of GH16–GH18 imply that flooding occurred in short-time succession (event-like) and abated around 300 years BP. Otherwise, the palaeomagnetic signals would be characterised by a strong West declination like in the very young sediments in OY profile (OY1–OY10; Fig. 5). Besides, OY profile represents a point bar position, and its alluvial units are not comparable with well-stratified floodplain deposits (a model of Medjerda floodplain evolution is going to be published in Zielhofer et al. (2004)).

## 5. Discussion

### 5.1. Abrupt mid-Holocene aridification: 4.7 ka collapse (Series 3a)

Sedimentation of coarse material covering the Neolithic soil points to an abrupt onset of fluvial activity in many profiles (G3, CH9, SA2, SS8b). It is the time of the beginning of the mid-Holocene aridification, which is associated with widespread sedimentation all over the Saharan region and substantial area of Mediterranean North Africa (Geyh and Jäkel, 1974; Rohdenburg, 1977; Sabelberg, 1977; Petit-Maire et al., 1997; Pachur, 1999; deMenocal et al., 2000; Pantaléon-Cano et al., 2003). Bourguou (1993) describes the formation of the first generation of clay dunes (lunettes) under drier conditions. Petit-Maire (1994) concluded that the lake levels in the western Saharan region dropped substantially until finally drying out. Roberts et al. (1994) and Lamb et al. (1995) come to similar conclusions, pointing to lake level falls in Tigmamine (Morocco). This was the time of human migration from the inner part of the Sahara towards southern regions (cf. Faust, 1989). In Tunisia some Libyan tribes settled in the Medjerda valley (Roubet, 1983). From this time on, we must assume an increasing influence of human activity in Tunisia on landscape evolution, so that morphodynamic change might have been triggered by human activity as well as by climate. However, we suppose that at that time climate dominated geomorphic processes, as the increase of the average sedimentation rate remains moderate (Fig. 4)—in comparison to historical times. In addition, Mediterranean pollen records and lake cores point to a climate-driven mid-Holocene aridification (Brun, 1992; Yll et al., 1997; Magri, 1999; Magri and Sadori, 1999; Ramrath et al., 2000).

The mid-Holocene Medjerda river aggradation ends with fine-grained sediments at the end of the fourth millennium BP (Fig. 4). Hydromorphic features within

clayey deposits (e.g. SA3, OM7) indicate a high ground water table at that time.

### 5.2. 3.0 ka event (Series 3b)

Medjerda floodplain sediments indicate a sudden change in fluvial dynamics around 3.0 ka cal BP (SA5, PJ8, CH9). The sedimentation rate increases for a short period of time (Fig. 4). Enhanced fluvial activity around 3.0 ka cal BP has not been clearly detected in North African alluvial records (e.g. Ballais, 1995). However, Stevenson et al. (1993) presented findings from Lac Ichkeul, which is situated about 100 km north-east of our investigation area, reporting aridification and, according to Rohdenburg's model, geomorphic activity at that time. A higher salinity and the appearance of *Phillyrea* in the pollen diagram suggest drier conditions at the beginning of the third millennium BP. In Western Andalusia a geomorphic accentuation is shown by aggradation of sandy deposits in still-water environments (Faust et al., 2000). Four years ago, we did not interpret our findings climatically because it was an isolated finding. But since Reed et al. (2001) described an abrupt desiccation phase nearby in the Laguna de Medina (Andalusia) around 3.0 ka cal BP, it is possible to relate the geomorphic change in Western Mediterranean to a drier climate. According to our additional findings from Northern Tunisia, a widespread 3.0 ka cal BP Western Mediterranean aridification becomes more apparent. This is documented from Portuguese coastal lagoons (Santos and Sánchez Goñi, 2003) and the Middle Atlas of Morocco (Lamb et al., 1995) as well. Probably, West Mediterranean aridification may be linked to temperature depressions in the North Atlantic region (cf. Bond et al., 2001; cf. Oppo et al., 2003).

### 5.3. Pre-Roman to Roman soil formation until 1700 cal BP (Series 3c)

Sediments from the Punic and especially Roman era represent landscape stability. Several profiles indicate fine sedimentation and subsequent soil formation (SS4, CH10, G6, GH2). The few palynological investigations only permit speculative statements about the climatic conditions in North Africa in the course of Antiquity: Stevenson et al. (1993) point to a stabilization phase of vegetation, probably due to more humid conditions at about 1.9 ka cal BP. According to our results, we assume that the onset of humid conditions must have begun somewhat earlier. By means of marine pollen profiles obtained from the Gulf of Gabes, Brun and Rouvillois-Brigol (1985) observe a gradual increase of oak pollen around 2.5 ka cal BP, which they interpret as evidence of a short period of humidity. Low sedimentation rates within the Medjerda alluvial record indicate stable fluvial dynamics during Antiquity and, therefore, support

the pollen record of the Gulf of Gabes. Is a slight increase in humidity sufficient to create geomorphic stability? Since at least 2.5 ka cal BP we can infer heightened Punic land use, enhanced after 146 BC by the Romans (Zielhofer and Faust, 2004). With the beginning of Roman times (e.g. Cherry, 1998), it is essential to include human impact when analysing palaeogeomorphic processes, as Roman activity not only reached coastal towns and their vicinities but also far into the hinterland. The main population areas were the fertile plains of the Medjerda (*Bagrada*) river and its surroundings (Hafemann, 1981). Land use intensity in these areas must have been comparable to modern times. Already in Punic times there was a dense cultivation of cereals in the Medjerda catchment area (Gabriel, 1984). During the so-called *Pax Romana* (Roman peace) there was a marked extension of the cultivation of olives. De Vos (2000) reveals intense olive cultivation in the headwaters of the Southern Medjerda tributaries at that time. Despite more intensive land use during the Roman period, our results (low sedimentation rates; Fig. 4) indicate geomorphic stability. We attribute this to agricultural methods used by the Roman in North Africa (terracing, irrigation, water retaining techniques, hedge plantings), which were in many ways adjusted to the natural conditions of the landscape (cf. White, 1970; cf. Barker, 1996).

Whether social behaviour affects morphodynamics has been debated for a long time (May, 1991; Faust, 1993; Zielhofer and Faust, 2004). Geomorphic stable and active periods frequently correlate with social prosperity and social crisis (Faust, 1993). Feedbacks arise where climate determines living conditions (Hsü, 2000). Within the tropics and subtropics, living conditions are worsened mainly because of water being in short supply. Hence, societies in these zones suffer more from the influence of declining precipitation than from changed temperatures (cf. Verschuren et al., 2000). Similar conclusions are applicable to landscapes. Their susceptibility to geomorphic activity (erosion and redeposition) rises with increasing aridity (up to a certain degree). Landscapes become ecologically (soil formation, vegetation cover, river incision) as well as socially (prospering agriculture, excess goods and resulting trade, security) more stable when humidity increases. However, climatic and anthropogenic impacts may not only intensify but also alleviate each other's effects.

#### 5.4. Late to post-Roman crisis from 1700 cal BP (Series 4a)

From the late Roman period we can assume that climatic as well as human impact forces enhanced geomorphic activity. This was a phase of major floods. The whole Medjerda basin is affected and

floodplain deposits occur in the Punic-Roman settlement area.

Marine pollen profiles of the Gulf of Gabes (Brun, 1992) present a more arid vegetation at that time, with *Artemisia* pollen leading to a peak between 1.5 and 1.0 ka cal BP. Consistent with the result of Brun (1992) is the analysis of Stevenson et al. (1993) in Northern Tunisia. *Quercus ilex* pollen, a bioclimatical indicator for drier conditions, appear and disturbance in the vegetation cover recommences at 1.4 ka cal BP. Stevenson et al. (1993) point to a higher salinity in the Lac Ichkeul (Northern Tunisia) after 1.5 ka cal BP. Hunt et al. (2001) suggest a steppic landscape in Western Libya that persisted until the early Arab period. Generally, more arid conditions in Northern Tunisia may correspond with Northern Hemisphere cooling periods during Late Quaternary (cf. Bond et al., 2001; Zielhofer et al., 2004). Likewise, Bond et al. (2001) document a Northern Hemisphere cooling event in late Antiquity. These disadvantageous climatic conditions coincide with the social decline in Mediterranean North Africa, starting with the invasion of the Vandals (cf. El Hadi Cherif, 1984). It is the time of the Great Migration of Nations during a climatic deterioration.

Post-Roman territorial conflicts have obviously led to an abandonment of terraces and a reduction of olive cultures on the slopes. Climatically reinforced, this may cause severe damage to the landscape. Consequently, heavy flooding appears at that time (Faust and Zielhofer, 2002). The transport of cobbles increased greatly and widespread aggradation terrace took place in Mediterranean North Africa. These sediments contain fragments of Roman pottery on nearly every site (Vita-Finzi, 1969; Ballais, 1995). After a brief slowdown in fluvial activity, our palaeomagnetic findings indicate another phase of enhanced fluvial dynamics around 1000 years BP (Fig. 5). This period correlates with the Oort sunspot minimum (cf. Fig. 4; Stuiver and Quay, 1980; Wigley and Kelly, 1990). Even a short-term variation in solar activity may induce changes in sensitive palaeoclimatic archives (cf. Schönwiese et al., 1994; Blackford and Chambers, 1995; Stuiver et al., 1997; Cioccale, 1999).

#### 5.5. Soil Formation between 0.9 and 0.7 ka cal BP (End of Series 4a)

The Medieval Warm Period (Schönwiese et al., 1994; Ballais, 1995; Le Houérou, 1996) corresponds with a period of geomorphic stability in North Tunisia, which is shown by the sedimentation of fine-grained deposits and weak humification within the Medjerda floodplain. The Medieval Warm Period was intensified by increased sunspot activity (cf. Fig. 4; Stuiver and Quay, 1980; Wigley and Kelly, 1990). Globally rising temperatures lead to more humidity in Mediterranean Tunisia. Severe

deforestation and further increase in agriculture disturb the vegetation, so that the possibilities for the palaeoclimatic interpretation of pollen diagrams are reduced. However, it is interesting that at around 0.8 ka cal BP the ostracod evidence indicates slightly less saline conditions in Lac Ichkeul, a fact which is also seen in the disappearance of the salinity indicator *Ammonia batava* (Stevenson et al., 1993). Ballais (1995) assumes that the Tunisian population was probably low at the beginning of the Hafsid period (12th century AD). This may support landscape stability at that time.

#### 5.6. Fine-grained sedimentation from 0.7 ka cal BP (Series 4b)

We observe increasing Medjerda sedimentation rates around 700 yr BP (Fig. 4). For this period only few North African palaeoclimatic records are available. Stevenson et al. (1993), from the close-by Lac Ichkeul, point to higher salinity, which is indicated by the occurrence of *Ammonia batava* and *Cyprideis torosa*. The salinity is accompanied by a reduction of the freshwater influx. On global scale, our enhanced sedimentation rates correlate with the Wolf and Spörer minimum (cf. Eddy, 1976; Stuiver et al., 1997).

In the mid-Medjerda valley the phase of fine-grained sedimentation concludes with a late Medieval soil formation (around 500 yr BP, Figs. 4 and 5). Probably, it corresponds to Camuffo's (1987) disruption of "Little Ice Age" in the Adriatic Sea (optimum between Spörer and Maunder minimum). The late Medieval soil formation is of short duration.

#### 5.7. Youngest Layer <400 yr BP (Series 5)

Starting at 400 yr BP, disastrous flood-events set in and lead to the aggradation of the laminated Youngest Layer in the mid-Medjerda basin (Fig. 4). Ballais (1995) describes a "very low post-Islamic terrace", which has been dated by radiocarbon to  $610 \pm 110$  BP. Referring to the far more arid regions of the Gulf of Gabes, this points to a somewhat earlier onset of morphodynamic activity. On global scale, the years between 1600 and 1830 AD, representing the Maunder minimum (Eddy, 1976), are the coldest ones of the Little Ice Age (Hsü, 2000).

On the basis of pollen records from Eastern Algeria, Ritchie (1984) detects the onset of present-day degradation conditions around 400 years BP. This result matches well with our findings from Northern Tunisia. Regrettably, Ritchie does not pay attention to the initiator of this development.

Afterwards, conflicts with the colonial power increased in the Medjerda region. Native farmers left large parts of the fertile Medjerda region to the colonial power and moved into the mountains (Faust, 1993).

Being unfamiliar with this mountain landscape, the farmers' inappropriate land use induced soil erosion. Above-average sedimentation rates (2.5 mm/year) can now be observed (Fig. 4).

## 6. Conclusions

### 6.1. Centennial scale alluvial record

Detailed morphostratigraphical field works, palaeomagnetism and radiocarbon dates allow a centennial scale record of Northern Tunisian fluvial sequences (Fig. 4). Alternating sediment texture, sedimentation rates and soil formation within Medjerda overbank deposits indicate short-term fluctuations in late Holocene fluvial dynamics. However, according to Vandenberghe et al. (1994), Vandenberghe (2002) and Kalis et al. (2003, p. 59) river systems do not always react to climatic shifts of short duration. The centennial to millennial duration of such climate oscillations may be too brief for changes in fluvial dynamics, due to longer response times of catchment areas in central Europe (Vandenberghe, 2002). In contrast, in the Mediterranean fluvial systems, like the Medjerda River changes in fluvial dynamics are recorded in short-term time scales of only a few centuries. This can also be observed in other alluvial deposits of semiarid to subhumid subtropics (Arnaud-Fassetta, 2002; Jenny et al., 2002; Macklin et al., 2002).

### 6.2. Bond events

High resolution records from marine cores in the North Atlantic region have given evidence for Late Pleistocene coolings over time periods of between  $10^3$  and  $10^4$  years (Heinrich, 1988; Bond et al., 1992, Bond et al., 1993; Bond and Lotti, 1995). These Heinrich events appear in marine cores of the subtropical Northeast Atlantic (Bard et al., 2000) and the West Mediterranean Sea (Cacho et al., 2000) as well as in central Mediterranean lake sediments (Allen et al., 1999).

Additionally, Bond et al. (1997, 2001) were able to prove North Atlantic coolings with a significantly shorter cyclicity of about 1450 years for the Holocene (Bond events). Furthermore, a few Holocene palaeoclimatic records point to the fact that cooler and drier conditions within the Mediterranean basin correspond to North Atlantic Bond events (Ramrath et al., 2000; Goy et al., 2003; Santos and Sánchez Goñi, 2003). The comparison of Medjerda sedimentation rates with the haematite curve of Bond et al. (2001) reveals a parallel progression of late Holocene North Atlantic cooling and increased alluviation in Mediterranean Tunisia (Fig. 4). We assume more arid conditions with enhanced fluvial dynamics around 4.7 ka, 3.0 ka, 1.6 ka and 0.4 ka. These



short-term periods of geomorphic activity match well with North Atlantic Bond events. The findings indicate a late Holocene climatic link between the North Atlantic region and the Mediterranean basin. Short-term climatic oscillations are clearly shown in computed sedimentation rates, proving the high sensitivity of the Medjerda river system. For this reason, Mediterranean alluvial archives may be very useful for palaeoclimatic reconstructions of high to moderate resolution.

### 6.3. *Man or climate?*

In central European river systems, short-term oscillations of Holocene flood plain deposits have been attributed to human impact in many cases (Litt, 1992; Barsch et al., 1993; Kalis et al., 2003). Thus, differences in the stratigraphical history of various river systems are due to regional settlement patterns rather than climate. In addition, many findings from palaeoclimatic archives in the central Mediterranean exhibit the dominant influence of man on geomorphic processes during the late Holocene (Shaw, 1981; Ramrath et al., 2000; Oldfield et al., 2003). However, the appraisal of human influence is problematic. For instance, intense land use may have contrasting effects on landscape depending on the applied land use system. Furthermore, social crisis as well as economic prosperity may have similar geomorphic effects (Hsü, 2000). Therefore, we may assume that anthropogenic stress was equally important during the entire study period in our investigation area. During phases of enhanced aridity man has accelerated fluvial activity (e.g. post-Roman crisis). However, climatic optima caused landscape stability regardless of the social situation. Our findings provide evidence that late Holocene Medjerda fluvial dynamics in Northern Tunisia were chiefly driven by climate. Anthropogenic impact intensified or attenuated geomorphic processes at most.

### Acknowledgements

We would like to thank the *Deutsche Forschungsgemeinschaft* (DFG) for supporting this project (FA 239/2-1 and FA 239/2-2). We wish to thank José Antonio Caro Gomez from the University of Seville for the evaluation of the artefacts and ceramics and Annette Kadereit (Heidelberg, Academy of Science) for the IRSL dating in OM profile. Furthermore, we are deeply grateful for the thin section analyses, conducted by Norbert Günster, and the evaluation of the molluscs by Ana Porras (University of Seville). For helpful comments, we are most thankful to Kevin White and an anonymous reviewer.

### References

- Allen, J.R.M., Brandt, U., Brauer, A., Hubberten, H.-W., Huntley, B., Keller, J., Kraml, M., Mackenson, A., Mingram, J., Negendank, J., Nowaczyk, N.R., Oberhänsli, H., Watts, W.A., Wulf, S., Zolitschka, B., 1999. Rapid environmental changes in southern Europe during the last glacial period. *Nature* 400, 740–743.
- Arnaud-Fassetta, G., 2002. Geomorphological records of a 'flood-dominated regime' in the Rhône Delta (France) between the 1st century BC and the 2nd century AD. What correlations with the catchment paleohydrology? *Geodinamica Acta* 15, 79–292.
- Baena Escudero, R., 1997. El paleomagnetismo: técnicas y aplicaciones a secuencias de travertinos y depósitos asociados. *Etudes de Géographie Physique* 26 (Suppl.), 103–106.
- Ballais, J.-L., 1995. Alluvial Holocene terraces in eastern Maghreb: climate and anthropogenic controls. In: Lewin, J., Macklin, M.G., Woodward, J.C. (Eds.), *Mediterranean Quaternary river environments*. Balkema, Rotterdam, pp. 183–194.
- Bard, E., Rostek, F., Turon, J.L., Gendreau, S., 2000. Hydrological impact of Heinrich events in the subtropical northeast Atlantic. *Science* 289, 1321–1324.
- Barker, G. (Ed.), 1996. *Farming the Desert (I)*. UNESCO Publications, Paris, 404pp.
- Barsch, D., Mäusbacher, R., Schukraft, G., Schulte, A., 1993. Die Änderungen des Naturraumpotentials im Jungneolithikum des nördlichen Kraichgau dokumentiert in fluvialen Sedimenten. *Zeitschrift für Geomorphologie NF Supplement* 93, 175–187.
- Blackford, J.J., Chambers, F.M., 1995. Proxy climate record for the last 1000 years from Irish blanket peat and a possible link to solar variability. *Earth and Planetary Science Letters* 133, 145–150.
- Bond, G.C., Lotti, R., 1995. Iceberg discharges into the North Atlantic on millennial time scales during the last glaciation. *Science* 267, 1005–1010.
- Bond, G.C., Heinrich, H., Broecker, W., Labeyrie, L., McManus, J., Andrews, J., Huon, S., Jantschik, R., Clasen, S., Simet, C., Tedesco, K., Klas, M., Bonani, G., Ivy, S., 1992. Evidence for massive discharges of icebergs into the North Atlantic Ocean during the last glacial period. *Nature* 360, 245–249.
- Bond, G.C., Broecker, S., Johnson, J., McManus, J., Labeyrie, L., Jouzel, J., Bonani, G., 1993. Correlations between climate records from North Atlantic sediments and Greenland ice. *Nature* 365, 143–147.
- Bond, G.C., Showers, W., Cheseby, M., Lotti, R., Almasi, P., deMenocal, P., Priore, P., Cullen, H., Hajdas, I., Bonani, G., 1997. A pervasive millennial-scale cycle in North Atlantic Holocene and Glacial climates. *Science* 278, 1257–1266.
- Bond, G.C., Kromer, B., Beer, J., Muscheler, R., Evans, M.N., Showers, W., Hoffmann, S., Lotti-Bond, R., Haidas, I., Bonani, G., 2001. Persistent solar influence on north Atlantic climate during the Holocene. *Science* 294, 2130–2136.
- Bourgou, M., 1993. Le bassin-versant du Kebir-Miliane (Tunisie Nord-orientale). Etude géomorphologique. Publications de la Faculté de Sciences Humaines et Sociales de Tunis, Série II 23, 435pp.
- Brun, A., 1992. Pollens dans les séries marines du Golfe de Gabès et du plateau des Kerkennah (Tunisie): Signaux climatiques et anthropiques. *Quaternaire* 3, 31–39.
- Brun, A., Rouvillois-Brigol, M., 1985. Apport de la Palynologie à l'Histoire du Peuplement en Tunisie. (ONRS) Palynologie archéologique II. Paris, pp. 215–226.
- Bucur, I., 1994. The direction of the terrestrial magnetic field in France during the last 21 centuries—Recent progress. *Physics of the Earth and Planetary Interiors* 87, 95–109.
- Cacho, I., Grimalt, J.O., Sierro, F.J., Shackleton, N., Canals, M., 2000. Evidence for enhanced Mediterranean thermohaline circulation during rapid climatic coolings. *Earth and Planetary Science Letters* 183, 417–429.

- Camuffo, D., 1987. Freezing of the Venetian lagoon since the 9th century AD in comparison to the climate in western Europe and England. *Climatic Change* 10, 43–66.
- Cherry, D., 1998. Frontier and society in Roman North Africa. Clarendon Press, Oxford 291pp.
- Cioccale, M.A., 1999. Climatic fluctuations in the Central Region of Argentina in the last 1000 years. *Quaternary International* 62, 35–47.
- Clark, A.J., Tarling, D.H., Noël, M., 1988. Developments in archaeomagnetic dating in Britain. *Journal of Archaeological Science* 15, 645–667.
- Dearing, J.A., Livingstone, I.P., Bateman, M.D., White, K., 2001. Palaeoclimate records from OIS 8.0–5.4 recorded in loess-palaeosol sequences on the Matmata Plateau, southern Tunisia, based on mineral magnetism and new luminescence dating. *Quaternary International* 76/77, 43–56.
- deMenocal, P., Ortiz, J., Guilderson, T., Adkins, J., Sarnthein, M., Baker, L., Yarusinsky, M., 2000. Abrupt onset and termination of the African Humid Period: rapid climate responses to gradual insolation forcing. *Quaternary Science Reviews* 19, 347–361.
- de Vos, M., 2000. Rus Africanum. Terra, acqua olio nell' Africa settentrionale. Scavo e ricognizione nei dintorni di Dougga, Alto Tell tunisino. Collana Labirinti 50, Trento, 200pp.
- El Hadi Cherif, M., 1984. Geschichte. In: Schliephake, K. (Ed.), Tunesien. Thienemann, Stuttgart, pp. 92–169.
- Eddy, J.A., 1976. The maunder minimum. *Science* 192, 1189–1202.
- Evans, M.E., 1996. Archeomagnetic results from the Mediterranean region—an overview. *Geological Society Special Publications* 105, 373–384.
- Faust, D., 1989. Gesteinsbedingte Relief- und Bodenentwicklung in den Monts Kabyè (N-Togo) und Auswirkungen auf den Agrarraum. *Zeitschrift für Geomorphologie N.F. Supplementband* 74, 57–69.
- Faust, D., 1993. Probleme des Ressourcenschutzes in Nordtunesien. *Geomethodica* 18, 113–128.
- Faust, D., 1995. Erkenntnisse zur holozänen Landschaftsentwicklung in der Campina Niederandalusiens. *Geoökodynamik* 16, 153–171.
- Faust, D., Zielhofer, C., 2002. Reconstruction of the Holocene water level amplitude of Oued Medjerda as an indicator for changes of the environmental conditions in Northern Tunisia. *Zeitschrift für Geomorphologie N.F. Supplementband* 128, 161–175.
- Faust, D., Diaz del Olmo, Baena Escudero, R., 2000. Soils in the Holocene alluvial sediments of the Rio Fraja valley, Spain: in situ or soil-sediments? *Catena* 41, 133–142.
- Gabriel, B., 1984. Vorgeschichte und Klimaentwicklung. In: Schliephake, K. (Ed.), Tunesien. Thienemann, Stuttgart, pp. 75–91.
- Gallet, Y., Genevey, A., Le Goff, M., 2002. Three millennia of directional variation of the Earth's magnetic field in western Europe as revealed by archeological artefacts. *Physics of the Earth and Planetary Interiors* 131, 81–89.
- Geyh, M., Jäkel, D., 1974. Spätpleistozäne und holozäne Klimageschichte der Sahara aufgrund zusätzlicher  $^{14}\text{C}$ -daten. *Zeitschrift für Geomorphologie N.F.* 18, 82–98.
- Giessner, K., 1984. Naturraum und landschaftsökologische Probleme. In: Schliephake, K. (Ed.), Tunesien. Thienemann, Stuttgart, pp. 23–74.
- Goy, J.L., Zazo, C., Dabrio, C.J., 2003. A beach-ridge progradation complex reflecting periodical sea-level and climate variability during the Holocene (Gulf of Almería, Western Mediterranean). *Geomorphology* 50, 251–268.
- Hafemann, D., 1981. Historische Geographie Nordafrikas (Tunesien, Algerien)—römische Kulturlandschaft um das Jahr 300 n. Chr. Afrika-Kartenwerk 15, Borntraeger, Berlin, 114pp.
- Heinrich, H., 1988. Origin and consequences of cyclic ice rafting in the Northeast Atlantic Ocean during the Past 130,000 years. *Quaternary Research* 29, 142–152.
- Hsü, K., 2000. Klima macht Geschichte. Orell Füssli, Zürich 334 pp.
- Hunt, C.O., Rushworth, G., Gilbertson, D.D., Mattingly, D.J., 2001. Romano-Libyan dryland animal husbandry and landscape: pollen and palynofacies analyses of coprolites from a farm in the Wadi El-Amud, Tripolitania. *Journal of Archaeological Science* 28, 351–363.
- Jenny, B., Valero-Garcés, B.L., Villa-Martinez, R., Urrutia, R., Geyh, M., Veit, H., 2002. Early to Mid-Holocene aridity in central Chile and the Southern Westerlies: the Laguna Aculeo Record (34°S). *Quaternary Research* 58, 160–170.
- Johnsen, S.J., Clausen, H.B., Dansgaard, W., Fuhrer, K., Grunestrup, N., Hammer, C.U., Iversen, P., Jouzel, J., Stauffer, B., Steffensen, J.P., 1992. Irregular glacial interstadials recorded in a new Greenland ice core. *Nature* 359, 311–313.
- Kalis, A.J., Merkt, J., Wunderlich, J., 2003. Environmental changes during the Holocene climatic optimum in central Europe—human impact an natural causes. *Quaternary Science Reviews* 22, 33–79.
- Knox, J.C., 1993. Large increases in flood magnitude in response to modest changes in climate. *Nature* 361, 430–432.
- Knox, J.C., 2000. Sensitivity of modern and Holocene floods to climate change. *Quaternary Science Reviews* 19, 439–457.
- Lamb, H.F., Gasse, F., Benkaddour, A., El Hamouti, N., van der Kaars, S., Perkins, W.T., Pearce, N.J., Roberts, C.N., 1995. Relation between century-scale Holocene arid intervals in tropical and temperate zones. *Nature* 373, 134–137.
- Le Houérou, H.N., 1996. Climate change, drought and desertification. *Journal of Arid Environments* 34, 133–185.
- Leser, H., 1977. Feld- und Labormethoden der Geomorphologie. Walter de Gruyter, Berlin, New York 446pp.
- Litt, T., 1992. Fresh investigations into the natural and anthropogenically influenced vegetation of the earlier Holocene in the Elbe-Saale region, central Germany. *Vegetation History and Archaeobotany* 1, 69–74.
- Macklin, M.G., Fuller, I.C., Lewin, J., Maas, G.S., Passmore, D.G., Rose, J., Woodward, J.C., Black, S., Hamlin, R.H.B., Rowan, J.S., 2002. Correlation of fluvial sequences in the Mediterranean basin over the last 200 ka and their relationship to climate change. *Quaternary Science Reviews* 21, 1633–1641.
- Magri, D., 1999. Late-Quaternary vegetation history at Lagaccione near Lago di Bolsena (central Italy). *Review of Palaeobotany and Palynology* 106, 171–208.
- Magri, D., Sadori, L., 1999. Late Pleistocene and Holocene pollen stratigraphy at Lago di Vico, central Italy. *Vegetation History and Archaeobotany* 8, 247–260.
- May, T., 1991. Morphodynamik und Bodenbildungen im westlichen Mittelraum seit dem mittleren Holozän—anthropogen oder klimatisch gesteuert? Theoretische Überlegungen und konkrete Beispiele. *Geographische Zeitschrift* 79, 212–229.
- Oldfield, F., 2000. Out of Africa. *Nature* 403, 370–371.
- Oldfield, F., Asoli, A., Accorsi, C.A., Mercuri, A.M., Juggins, S., Langone, L., Rolph, T., Trincardi, F., Wolff, G., Gibbs, Z., Vigliotti, L., Frignani, M., van der Post, K., Branch, N., 2003. A high-resolution late Holocene palaeoenvironmental record from the central Adriatic Sea. *Quaternary Science Reviews* 22, 319–342.
- Oppo, D.W., McManus, J.F., Cullen, J.L., 2003. Deepwater variability in the Holocene epoch. *Nature* 422, 277–278.
- Pantaléon-Cano, J., Yll, E.-I., Pérez-Obiol, R., Roure, M., 2003. Palynological evidence for vegetational history in semi-arid areas of the western Mediterranean (Almería, Spain). *The Holocene* 13, 109–119.
- Pachur, H.-J., 1999. Paläo-Environment und Drainagesysteme der Ostsahara im Spätpleistozän und Holozän. In: Klitzsch, E., Thorwehe, U. (Eds.), Nordost-Afrika: Strukturen und Ressourcen. Wiley-VCH, Weinheim, pp. 366–445.
- Petit-Maire, N., 1994. Natural Variability of the Asian, Indian and African Monsoons over the last 130 ka. In: Desbois, M.,

- Désalmand, A. (Eds.), *Global Precipitation and Climate Change*. NATO ASI Series 126. Springer, Berlin, Heidelberg, pp. 3–26.
- Petit-Maire, N., Beaufort, L., Page, N., 1997. Holocene climate change and man in the present-day Sahara. In: Dalfes, N., Kukla, G., Weiss, H. (Eds.), *Third Millennium BC Climate Change and Old World Collapse*. Springer, Berlin, Heidelberg, pp. 297–308.
- Ramrath, A., Sadori, L., Negendank, F.W., 2000. Sediments from Lago di Mezzano, central Italy: a record of Lateglacial/Holocene climatic variations and anthropogenic impact. *The Holocene* 10, 87–95.
- Reed, J.M., Stevenson, A.C., Juggins, S.J., 2001. A multi-proxy record of Holocene climate change in southwestern Spain: the Laguna de Medina, Cadiz. *The Holocene* 11, 707–719.
- Ritchie, J.C., 1984. Analyse pollinique de sédiments holocènes supérieures des hauts plateaux du Maghreb oriental. *Pollen et Spores* 26, 489–496.
- Roberts, N.F., Lamb, H.F., El Hamouti, N., Barker, P., 1994. Abrupt Holocene hydroclimatic events: palaeolimnological evidence from North-West Africa. In: Millington, A.C., Pye, K. (Eds.), *Environmental change in drylands: biogeographical and geomorphological perspectives*. Wiley, Chichester, pp. 164–174.
- Rohdenburg, H., 1977. Neue  $^{14}\text{C}$ -Daten aus Marokko und Spanien und ihre Aussagen für die Relief- und Bodenentwicklung im Holozän und Jungpleistozän. *Catena* 4, 215–228.
- Rohdenburg, H., 1989. Landscape ecology—Geomorphology. Catena, Reiskirchen, 177pp.
- Rose, J., Meng, X., Watson, C., 1999. Palaeoclimate and palaeoenvironmental responses in the western Mediterranean over the last 140 ka: evidence from Mallorca, Spain. *Journal of Geological Society* 156, 435–448.
- Roubet, C., 1983. Une économie pastorale, pré-agricole en Algérie orientale: Le néolithique de tradition capsienne. *L'Anthropologie* 82, 583–586.
- Sabelberg, U., 1977. The stratigraphic record of late quaternary accumulation series in South West Morocco and its consequences concerning the pluvial hypothesis. *Catena* 4, 209–214.
- Santos, L., Sánchez Goñi, M.F., 2003. Lateglacial and Holocene environmental changes in Portuguese coastal lagoons 3: vegetation history of the Santo André coastal area. *The Holocene* 13, 459–464.
- Schönwiese, C.-D., Ullrich, R., Beck, F., Rapp, J., 1994. Solar signals in global climatic change. *Climatic Change* 27, 259–281.
- Semmel, A., 1989. Paleopedology and geomorphology: examples from the western part of central Europe. *Catena* 16 (Suppl.), 143–162.
- Shaw, B.D., 1981. Climate, environment, and history: the case of Roman North Africa. In: Wigley, T.M.L., Ingram, M.J., Farmer, G. (Eds.), *Climate and History—Studies in past climates and their impact on man*. Cambridge University Press, Cambridge, New York, Melbourne, pp. 379–403.
- Stevenson, A.C., Phethean, S.J., Robinson, J.E., 1993. The palaeosalinity and vegetational history of Garaet el Ichkeul, northwest Tunisia. *The Holocene* 3, 201–210.
- Stuiver, M., Quay, P.D., 1980. Changes in atmospheric carbon-14 attributed to a variable sun. *Science* 207, 11–19.
- Stuiver, M., Braziunas, T.F., Grootes, P.M., Zielinski, G.A., 1997. Is there evidence for solar forcing of climate in the GISP2 oxygen isotope record? *Quaternary Research* 48, 259–266.
- Stuiver, M., Reimer, P.J., Bard, E., Beck, J.W., Burr, G.S., Hughen, K.A., Kromer, B., McCormac, F.G., Plicht, J., Spurk, M., 1998. INTCAL 98 radiocarbon age calibration, 24,000 to 0 cal BP. *Radiocarbon* 40, 1041–1083.
- Tanguy, J.-C., Bucur, I., Thompson, J.F.C., 1985. Geomagnetic secular variation in Sicily and revised ages of historic lavas from Mount Etna. *Nature* 318, 453–455.
- Tanguy, J.-C., Le Goff, M., Principe, C., Arrighi, S., Chillemi, V., Paiotti, A., La Delfa, S., Patanè, G., 2003. Archeomagnetic dating of the Mediterranean volcanics of the last 2100 years: validity and limits. *Earth and Planetary Science Letters* 211, 111–124.
- Vandenberghe, J., 2002. The relation between climate and river processes, landforms and deposits during the Quaternary. *Quaternary International* 91, 17–23.
- Vandenberghe, J., Kasse, C., Bohncke, S., Kozarski, S., 1994. Climate-related river activity at the Weichselian–Holocene transition: a comparative study of the Warta and Maas rivers. *Terra Nova* 6, 476–485.
- Verschuren, D., Laird, K.R., Cumming, B.F., 2000. Rainfall and drought in equatorial east Africa during the past 1100 years. *Nature* 403, 410–414.
- Vita-Finzi, C., 1969. *The Mediterranean Valleys. Geological Changes in Historical Times*. Cambridge University Press, Cambridge 433pp.
- White, K.D., 1970. *Roman Farming*. Thames and Hudson, London 536pp.
- White, K., Drake, N., Millington, A., Stokes, S., 1996. Constraining the timing of alluvial fan response to Late Quaternary climatic changes, southern Tunisia. *Geomorphology* 17, 295–304.
- Wigley, T.M.L., Kelly, P.M., 1990. Holocene climatic change,  $^{14}\text{C}$  wiggles and variations in solar irradiance. *Philosophical Transactions of the Royal Society of London A330*, 547–560.
- Yll, E.-I., Perez-Obiol, R., Pantaléon-Cano, J., Roure, J.M., 1997. Palynological evidence for climatic change and human activity during the Holocene on Minorca (Balearic Islands). *Quaternary Research* 48, 339–347.
- Zielhofer, C., Faust, D., 2004. Morphodynamics around 12 and 2 ka cal BP in the middle course of the Oued Medjerda near Chemtou (Northern Tunisia). In: Howard, A.J., Macklin, M.G., Passmore, D.G. (Eds.), *The Alluvial Archaeology of NW Europe and the Mediterranean*. Balkema, Rotterdam, in press.
- Zielhofer, C., Faust, D., Diaz del Olmo, F., Baena, R., 2002. Sedimentation and soil formation phases in the Ghardimaou basin (Northern Tunisia) during the Holocene. *Quaternary International* 93–94, 109–125.
- Zielhofer, C., Faust, D., Baena Escudero, R., Diaz del Olmo, F., Kadereit, A., Moldenhauer, K.-M., Porras, A., 2004. Centennial-scale late Pleistocene to mid-Holocene synthetic profile of the Medjerda valley (Northern Tunisia). *The Holocene* 14, in press.
- Zolitschka, B., 1998. Paläoklimatische Bedeutung laminierter Sedimente—Holzmaar (Eifel, Deutschland), Lake C2 (Nordwest-Territorien, Kanada) und Lago Grande di Monticchio (Basilikata, Italien). *Relief Boden Paläoklima* 13, 1–176.